Transactions of the Materials Research Society of Japan 30[2] 565-570 (2005)

Quantum Phenomena in Surface-passivated Metallic Nanoparticles Studied by Photoelectron Spectroscopy

Akinori Tanaka
Department of Mechanical Engineering, Faculty of Engineering, Kobe University, 1-1 Rokkodai-cho, Nada-ku, Kobe 657-8501, Japan
Fax: 81-78-803-6123, e-mail: a-tanaka@mech.kobe-u.ac.jp

We have carried out the various photoemission studies of alkanethiolate- (AT-) passivated metallic (Ag and Au) nanoparticles supported on the highly oriented pyrolytic graphite (HOPG) substrates. From the detailed ultraviolet photoemission measurements, it is found that the Fermi-level onsets in the photoemission spectra of AT-passivated metallic nanoparticles on the HOPG substrates are not the metallic Fermi-edge, with the steep slope being away from the Fermi-level. Moreover, it is found that the core-level photoemission spectra shift to higher binding energy with decreasing the nanoparticle diameter. We attribute these unusual spectral features to the dynamic final-state effect in photoemission, indicative of the interaction between the nanoparticle and substrate through the surface-passivants on a femtosecond timescale. In order to investigate the excited-electron dynamics in surface-passivated metallic nanoparticles, we have carried out the femtosecond interferometric time-resolved two-photon photoemission studies of AT-passivated Ag nanoparticles on the HOPG substrates. The derived energy relaxation times are significantly larger than that of the bulk Ag crystallite. Moreover, it is found that the both decays of intermediate states (single-particle excitation) and plasmon (collective excitation) contribute to the experimental two-pulse correlation. From these results, we discuss the various quantum phenomena in the surface-passivated metallic nanoparticles.
Key words: Surface-passivated nanoparticle, Photoelectron spectroscopy, Electronic structure, Nanoparticle-substrate interaction, Ultrafast electron dynamics

1. INTRODUCTION

Metallic nanoparticles are attracting much interest from the viewpoints of both fundamental and device physics, since they show the distinctive physical and chemical properties found in neither bulk nor molecular/atomic systems, such as high catalytic activity[1] and Coulomb blockade.[2] Recently, the surface-passivated metallic nanoparticles have been chemically synthesized in the solution including surfactants.[3,4] These surface-passivated nanoparticles are monodisperse and very stable at room temperature, therefore, these are suitable to characterize their fundamental size-dependent properties. Furthermore, these surface-passivated nanoparticles exhibit the closed-packed nanoparticle self-assemblies on the single-crystalline substrates[5,6] therefore, it is considered that they could be important constituents of future nanostructured devices, such as single electron device, catalyst, and ultra highly density memory. In order to elucidate their detailed intriguing properties and to develop the future devices, it is indispensable to understand the interactions with the substrates supporting the nanoparticles as well as their electronic structures.

On the other hand, the transient dynamics of hot-electrons created by photoexcitation play an important role in the various physical and chemical phenomena. The excited electrons relax through a number of decay processes, such as electron-electron scattering, electron-phonon scattering, and electron-impurity/defect scattering. The detailed understanding of excited electron dynamics will provide not only information about the fundamental interactions in the many-body systems but also knowledge of the various optical, physical and chemical processes. Therefore, it is also indispensable to understand the excited-electron dynamics.

In this work, we report the results of various photoelectron spectroscopies for alkanethiolate- (AT-) passivated metallic (Ag and Au) nanoparticles supported on the HOPG substrates. From the discussions regarding the final-state effects on the photoemission spectra in the vicinity of Fermi level and core-level photoemission spectra, especially we will discuss the nanoparticle-substrate interactions through the surface-passivants of AT-passivated metallic nanoparticles on the HOPG substrates. From the femtosecond interferometric time-resolved two-photon photoemission (ITR-2PPE) spectra, we discuss the excited-electron dynamics in the surface-passivated metallic nanoparticles.

2. EXPERIMENT

The AT-passivated Ag nanoparticles were synthesized by two-phase reduction method.[3] The detailed procedure is described elsewhere.[7] The AT-passivated Au nanoparticles were synthesized by the method developed by Lin *et al.*[8] Firstly, 156 mg of didodecyldimethyl-ammonium (98 %) was added to 15 ml of toluene (99 %) and 24 μl of deionized water in order to form a 0.0225 M inverse micelle system. After that, 50 mg gold chloride (99.99%) was dissolved to this micelle solution by sonication for 15 minutes. After 54 μl of 9.4 M $NaBH_4$ (98 %) aqueous solution was added to the

above solution with stirring, Au nanoparticles were obtained. After 0.4 ml of alkanethiols (octanethiol (OT), dodecanethiol (DT), and hexadecanethiol (HDT)) (98 %) was added as a surface passivants, Au nanoparticles were precipitated with 7 ml of ethanol (99.5 %) and the bottom precipitates were dried under the vacuum. Then the dried precipitates were redispersed in 5 ml of toluene. The product was diluted in 15 ml of boiling toluene and was left 1 day. The toluene/nanoparticle-rich phase was corrected and was evaporated in a rotary evaporator, and then was washed with ethanol to remove the excess alkanethiol and reaction byproducts. After that, the product was redispersed in toluene, and finally the highly monodispersed AT-passivated Au nanoparticles were obtained. The size distributions in diameter and shapes of the synthesized AT-passivated Ag and Au nanoparticles were characterized by *ex-situ* observations with transmission electron microscope (TEM). As a further characterization, the optical measurements were performed.

Ultraviolet photoemission spectroscopy (UPS) measurements were performed with the He I resonance line ($h\nu$=21.2 eV) as the excitation source at 40 K. The core-level photoemission measurements using synchrotron-radiation (SR) were carried out at BL-5U of UVSOR Facility, Institute for Molecular Science, Okazaki, Japan. SR-photoemission measurements were performed with the incident photon energy of 180 eV at room temperature. The femtosecond interferometric time-resolved two-photon photoemission measurements were performed with a self-made Ti:sapphire oscillator using negative dispersion mirrors for dispersion compensation, at Department of Physics and Astronomy, University of Pittsburgh, USA. The output of fundamental light from the Ti:sapphire laser has a pulse width of about 10 fs, a wavelength of about 800 nm, and a repetition frequency of 90 MHz. The second harmonic light was generated by using a 80 μm-thick beta barium borate crystal, and the negative dispersion mirrors were used for group velocity dispersion compensation of the frequency-doubled light. The frequency-doubled light was divided into two beams with equal intensities by a beam splitter. One beam was used as a pump pulse to generate the excited-electrons, while the other beam was used as a probe pulse to photoemit the excited-electrons. For the all photoemission measurements, the synthesized AT-passivated Ag and Au nanoparticles were supported on the HOPG substrates by evaporating the solvent (toluene) from the dispersion of AT-passivated Ag and Au nanoparticles on the single-crystalline HOPG cleaved-surface in a nitrogen-filled glove bag directly connected to the ultrahigh-vacuum photoelectron spectrometer. Then the samples were transferred into the photoemission analysis chamber without exposure to air.

3. RESULS AND DISCUSSION

3.1 UPS in the vicinity of Fermi level.

Figure 1 shows the UPS spectra in the vicinity of Fermi level (E_F) of the DT-passivated Ag nanoparticles on the HOPG substrates and bulk Ag polycrystalline evaporated film. From the TEM observations, the monolayer of the DT-passivated Ag nanoparticle is considered to be formed on the HOPG substrate in the present samples for photoemission measurements. As shown in Fig. 1, while the photoemission spectrum in the vicinity of E_F of bulk Ag polycrystallite shows the metallic Fermi-edge, the Fermi-level onsets in the photoemission spectra of all the present DT-passivated Ag nanoparticles do not exhibit the usual metallic Fermi-edge, with the steep slope being away from the E_F. Moreover, the slopes of the leading edges are different from that of metallic Fermi-edge observed for bulk Ag crystallite, and depend on the nanoparticle diameters. The present photoemission spectra include the both contributions from DT-passivated Ag nanoparticles and HOPG substrates, because there is an uncovered region of DT-passivated Ag nanoparticles on the HOPG substrates in the present samples. However, since the photoemission spectrum in the vicinity of E_F of HOPG substrate exhibits the featureless shape reflecting the vanishing semimetallic density of states toward the E_F, the observed spectral features of DT-passivated Ag nanoparticles on the HOPG substrates are not caused by the HOPG substrates but are characteristic of Ag nanoparticles. When the lateral coverage of DT-passivated Ag nanoparticles on the HOPG substrate changes, the relative intensity of spectral feature from DT-passivated Ag nanoparticle to background intensity derived from the HOPG substrate change, but the spectral features derived from DT-passivated Ag nanoparticles shown no change. In general, the photoemission spectra reflect the change in the electronic structure of the samples (initial state effect) and final state effect originating from positively charged photohole created by the photoionization.[9-12] On the other hand, the optical extinction spectra of all the present DT-passivated Ag nanoparticles exhibit the distinctive Mie plasmon resonance around 3 eV in photon energy for all diameters, indicative of a collective motion of valence electrons typical for a metallic materials. Therefore, the observed spectral features in

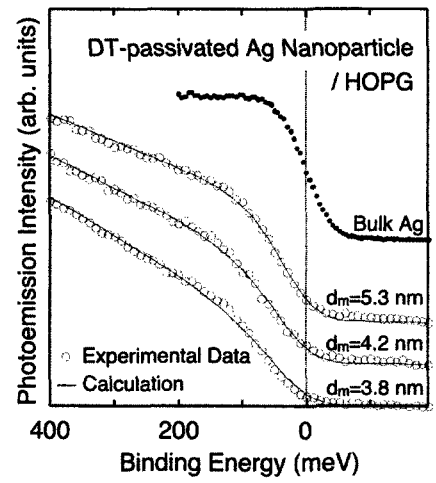

Fig. 1. Comparison of the experimental photoemission spectra of DT-passivated Ag nanoparticles with mean diameters of 3.8, 4.2, and 5.3 nm with the calculated ones based on the dynamic final-state effect model (see text). Open circles and solid lines show the experimental photoemission spectra and the fits to the experimental spectra, respectively. The top spectrum shows the Fermi-level onset observed for bulk Ag polycrystalline evaporated film for a comparison.

the vicinity of E_F are not due to the initial-state effect originating from the change in the electronic structure. It is considered that these unusual spectral features in the vicinity of E_F originate from the final-state effect due to the photohole remaining in the nanoparticles during the photoemission process. When the high-energy light such as vacuum ultraviolet light and X-ray excites a photoelectron, the photohole remaining in the nanoparticles during the time scale relevant to photoemission process will lower the kinetic energy of photoelectrons through the Coulomb interaction. Although the relaxation response within the nanoparticle may otherwise proceed normally, an excess positive charge remaining in the nanoparticle induces the final-state effect in the photoemission.[9-12] It is considered that this final-state effect would play a more important role in the present surface-passivated nanoparticles supported on the substrates, since the surface-passivated nanoparticle weakly couple with the substrates through the surface-passivant molecules. In the case of static charging, the kinetic energy shift of photoelectrons due to the photohole in the nanoparticle is give by $\Delta E=e^2/2C$, where $C=4\pi\varepsilon_0 R$ is the self-capacitance of the nanoparticle with a radius of R. An exact calculation shows that this energy-shift is given by $\Delta E=\alpha e^2/4\pi\varepsilon_0 R$ with α=0.41 for Ag nanoparticle.[8] In the case of photoemission, the nanoparticles are limited to have only positive charge (photohole), but the origin of this final-state effect on photoemission process should be same as that of single electron tunneling.

In order to theoretically describe these experimental results, we analyzed these photoemission spectra in the vicinity of E_F of DT-passivated Ag nanoparticles using a dynamic final-state effect model[7,10,11] that takes into account the Coulomb interaction between the photoelectron and photohole with a finite lifetime during the photoemission process. This detailed theoretical expression is described elsewhere.[7,10,11] In short, we assume the probability of photohole neutralization,

$$P(t)dt=(1/\tau)\exp(-t/\tau)dt, \qquad (1)$$

with a characteristic time τ that determined by the coupling strength between the nanoparticle and substrate. With the Coulomb potential acting on the photoelectron due to the photohole from the nanoparticle to infinity is expressed by $W(r)=\alpha e^2/4\pi\varepsilon_0$ $(1/R\text{-}1/r)$, where r is the distance from the center of the nanoparticle, the energy-shift after a time t for the photoelectron with a velocity v is described by $W(R+vt)$. The observed photoemission spectra average over a large number of photoelectrons at the different times t, therefore, this leads to the distribution of energy-shifts given by,

$$P(W)dW=\frac{CW_{max}}{(W_{max}-W)^2}\exp\left(-\frac{CW}{W_{max}-W}\right)dW, \qquad (2)$$

where $C=R/v\tau$ and $W_{max}=\alpha e^2/4\pi\varepsilon_0 R$ is maximum shift in the case of $t\rightarrow\infty$. The photoemission spectrum in the vicinity of E_F for nanoparticle with a radius of R, as a function of binding energy E_B, $S(E_B,R)$, can be described by the convolution of Fermi-Dirac function at relevant temperature and the energy-shift distribution function $P(W)$ in Eq. (2). Moreover, the experimental photoemission spectra include the contribution from the inhomogeneous width due to the size distribution, since $S(E_B,R)$ depends on a nanoparticle radius R through the size-dependent energy-shift distribution function $P(W)$. In addition, the present photoemission spectra include the contributions from a finite instrumental width and the photoemission intensity from uncovered region of HOPG substrate. Thus calculated fitting lines to the experimental spectra by the least-squares method are also shown by solid lines in Fig. 1. As shown in Fig. 1, these fitting lines based on the dynamic final-state effect model reproduce the experimental spectra for all diameters fairly well. From these calculations, the obtained parameters τ of the DT-passivated Ag nanoparticles on the HOPG substrates are 0.20×10^{-15} sec, 0.21×10^{-15} sec, 0.25×10^{-15} sec for the mean diameters of 3.8, 4.2, and 5.3 nm, respectively. It is concluded that the observed spectral features for DT-passivated Ag nanoparticles on the HOPG substrates can be explained with the dynamic final-state effect model and reflect the nanoparticle and substrate interactions through the surface-passivants on a femtosecond timescale. The lifetimes τ of the photohole directly correspond to the tunneling times through the surface-passivants of DT molecules. From the analogy of the single electron tunneling, these photohole lifetimes τ can be estimated to $\tau=R_tC_s$, where R_t is the tunnel resistance between the nanoparticle and substrate through the surface-passivants, and C_s is the self-capacitance of the nanoparticle. Therefore, the present discussions will provide the knowledge about the single electron tunneling in the nanoparticle/tunneling gap (surface-passivant molecule)/substrate system.

In order to investigate the surface-passivant dependence of this nanoparticle-substrate interaction, we have performed the photoemission study of Au nanoparticles passivated by the various AT (OT, DT, and HDT) molecules. Figure 2 shows the UPS spectra in the vicinity of E_F of various AT-passivated Au nanoparticle with mean diameters of 4 nm on the HOPG substrates. These

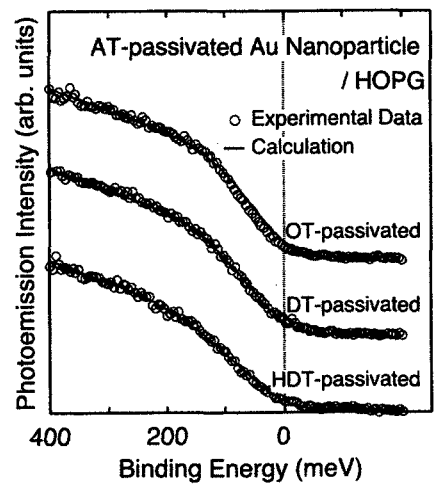

Fig. 2. Comparison of the experimental photoemission spectra at 40 K of OT-, DT-, and HDT-passivated Au nanoparticles with the mean diameters of 4 nm with the calculated ones based on the dynamic final-state effect model. Open circles and solid lines show the experimental photoemission spectra and the fits to the experimental spectra, respectively.

photoemission spectra also exhibit the spectral features reflecting the dynamic final-state effect as described above. An important point to note is that the slopes of the leading edges depend on the surface passivants. Using the same theoretical procedure as the above discussion, we have carried out a fit to the experimental spectra of the various AT-passivated Au nanoparticles in Fig. 2 by the least-squares method. The fitting lines to the experimental spectra are shown by solid lines in Fig. 2. As shown in Fig. 2, these fitting lines that take into account the dynamic final-state effect reproduce the experimental spectra for all samples fairly well. From these calculations, the obtained parameters τ of the OT-, DT-, and HDT-passivated Au nanoparticles supported on the HOPG substrates are 0.27×10^{-15} sec, 0.32×10^{-15} sec, 0.41×10^{-15} sec, respectively. It is concluded again that the observed spectral features for AT-passivated Au nanoparticles on the HOPG substrates can be explained with the dynamic final-state effect model and reflect the nanoparticle and substrate interactions through the surface-passivants on a femtosecond timescale. Moreover, it is found that these obtained parameters τ exponentially depend on the half of the interparticle distance between the neighboring nanoparticle (not give here). Here, the half of the interparticle distance corresponds to the distance between the Au nanoparticle and HOPG substrate, and is proportional to surface-passivant molecular length. As described above, the lifetimes τ of the photohole directly correspond to the tunneling times through the surface-passivants of AT molecules. From the analogy of the single electron tunneling, these photohole lifetimes τ can be estimated to $\tau=R_tC_s$. In this experiment, the nanoparticle diameters are same, and therefore C_s is same among three samples. It is considered that the surface-passivants dependent photohole lifetimes reflect the tunneling resistance between the nanoparticle and substrate. The tunneling resistance R_t is expressed by $R_t \propto \exp(\beta s)$, where β is the decay constant of the transconduction and s is the interelectrode separation that corresponds to the distance between the Au nanoparticle and HOPG substrate in this experiment. Therefore, it is concluded that the present surface-passivants dependence of photohole lifetime τ can be explained with the dependence of tunneling resistance on the distance between the nanoparticle and substrate.

3.2 Core-level photoemission spectra using SR

Figure 3(a) shows synchrotron-radiation Au $4f_{7/2}$ core-level photoemission spectra of DT-passivated Au nanoparticles with the various mean diameters d_m on the HOPG substrates at room temperature measured with photon energy of $h\nu$=180 eV, compared with that of bulk Au polycrystalline evaporated film. Figure 3(a) also shows the results of line-shape analyses for Au $4f_{7/2}$ core-level spectra of DT-passivated Au nanoparticles and bulk Au crystallite. Each decomposed peak was described by a convolution of Doniach-Sunjic line shape with a Gaussian due to the instrumental and phonon broadening. As well known, the components with higher binding energy and lower binding energy in the Au $4f$ core-level photoemission spectrum of bulk Au crystallite are bulk and surface components, respectively.[13] On the other hand, as shown in Fig. 3(a), it is found that the Au $4f$ core-level photoemission spectra of DT-passivated Au nanoparticles on the HOPG substrates are also represented by two components. As shown in Fig. 3(a), the relative intensity of higher binding energy component to lower binding energy component increases with decreasing the nanoparticle diameter. The nanoparticle systems have a higher number ratio of surface atoms to atoms in bulk with decreasing the nanoparticle diameter. Furthermore, the binding energy and spectral feature of the lower binding energy component in each sample are similar to those of bulk component in the Au $4f$ core-level photoemission spectrum observed for bulk Au crystallite. Therefore, it is concluded that the components with lower binding energy and higher binding energy in Au $4f$ core-level spectra of DT-passivated Au nanoparticles originate from the inner Au atoms of Au nanoparticles (bulk component) and the surface Au atoms of Au nanoparticles bonded to surface-passivants of

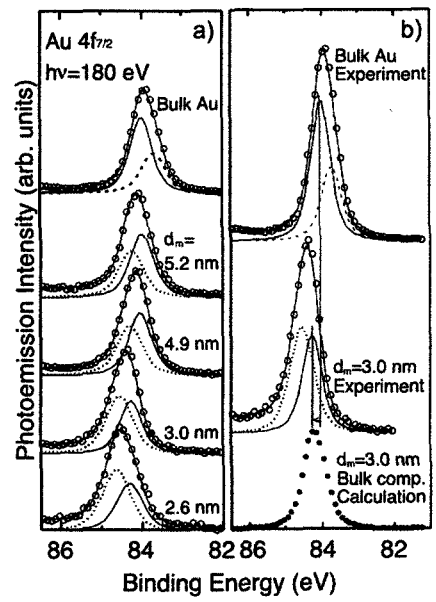

Fig. 3. (a) SR Au $4f_{7/2}$ core-level photoemission spectra of DT-passivated Au nanoparticles on the HOPG substrates at room temperature measured with photon energy of $h\nu$=180 eV. The observed spectrum of bulk Au crystallite is decomposed into bulk (solid line) and surface (dashed line) components, and those of DT-passivated Au nanoparticles on the HOPG substrates are decomposed into bulk components (solid lines) and surface components bonded to surface DTs (dotted lines). (b) Comparison of the experimental bulk component of DT-passivated Au nanoparticle with mean diameter of 3 nm on the HOPG substrate with the calculated one based on the dynamic final-state effect model. The top spectra show the experimental spectrum (open circle) and the corresponding decomposed components (solid line: bulk component, dashed line: surface component) of bulk Au crystallite. The middle spectra show the experimental spectrum (open circle) and the corresponding decomposed components (solid line: bulk component, dotted line: surface component) of DT-passivated Au nanoparticle with mean diameter of 3 nm on the HOPG substrate. The bottom spectrum shows the calculated bulk component based on the dynamic final-state effect model

DT molecules (surface component), respectively. From the detailed line-shape analyses, the chemical shifts of surface components with the mean diameters of 5.2, 4.9, 3.0, 2.6 nm are 0.27, 0.27, 0.28, and 0.33 eV, respectively. The chemical shifts of surface Au atoms bonded to DT molecules increase with decreasing the nanoparticle diameter. This indicates that the bonding nature between the surface-passivants of DT molecules and Au nanoparticle surface, such as a coordination number and configuration of surface-passivants, changes with the nanoparticle diameter. The above dependence of bonding nature on the nanoparticle diameter might originate from the structural factor such as size-dependent curvature of nanoparticle surface, effect due to the existence of habit in the smaller nanoparticles, *etc.* Here, an important point to note is that the bulk components of the DT-passivated Au nanoparticles on the HOPG substrates shift to higher binding energy side with decreasing the nanoparticle diameter. From the above discussion, the higher binding energy shifts of bulk components in the present DT-passivated Au nanoparticles on the HOPG substrates with decreasing the nanoparticle diameter are considered to originate from the final-state effect on the photoemission process. In order to analyze the present Au 4*f* core-level photoemission spectra, we apply the dynamic final-state model to Au 4*f* core-level photoemission spectra again. From a fit to UPS spectrum in the vicinity of E_F of the corresponding samples using the above dynamic final-state effect model, firstly we can derive the parameter C in the case of UPS, C_{UPS}. Then, we have transformed the parameter $C_{180\ eV}$ and have calculated the energy shift distribution function $P_{180\ eV}(W)$ using Eq. (2), in the case of Au 4*f* core-level photoemission measured with photon energy of $h\nu$=180 eV. From the analogy of the Fermi-level onset, the bulk component in Au 4*f* core-level spectrum of DT-passivated Au nanoparticle on the HOPG substrate can be theoretically described by the convolution of the bulk component observed for bulk Au crystallite with the above energy shift distribution function $P_{180\ eV}(W)$. In this calculation, we have taken into account the contribution from the inhomogeneous width due to the size distribution. Figure 3(b) shows the comparison of experimental bulk component in the Au $4f_{7/2}$ core-level spectrum of DT-passivated Au nanoparticles with mean diameter of 3 nm on the HOPG substrates with the calculated one from the experimental bulk component of bulk Au crystallite using dynamic final-state effect model. As shown in Fig. 3(b), the calculated bulk component reproduces the experimental one of DT-passivated Au nanoparticle on the HOPG substrate fairly well. Therefore, it is concluded that the experimental core-level photoemission spectral features of the present DT-passivated Au nanoparticles on the HOPG substrates can be also quantitatively characterized by the dynamic final-state effect model and can be described by the same parameters as the UPS spectra in the vicinity of E_F. Furthermore, this indicates that the present spectral feature reflects the nanoparticle and substrate interactions through the surface passivants of DT molecules on a femtosecond time scale. In the case of photoelectron excitation by photon with $h\nu$=180 eV, the electron from the Au $4f_{7/2}$ core-level is photoemitted with a kinetic energy of about 92 eV, corresponding to a velocity of v=5.7×10^6 m/sec. Since the photoelectron with this velocity travels the distance with the same order as nanoparticle radius on this femtosecond time scale, the dynamic final-state effect also exhibits in the core-level photoemission spectra. The present discussions will provide the knowledge about the single electron tunneling in the nanoparticle/[surface-passivants (tunneling-gap)]/substrate system. However, in order to quantitatively discuss the single electron phenomena from these final-state effects on core-level photoemission, a more rigorous calculation, detailed size-dependence, and the detailed comparison with the tunneling microscopic experiments would be necessary.

3.3 ITR-2PPE spectra

Figure 4 shows the two-photon photoemission (2PPE) spectrum of the octadecanethiolate- (ODT-) passivated Ag nanoparticles on the HOPG substrate with d_m=4.4 nm measured with photon energy of 3.1 eV at zero pump-probe delay, compared with that of HOPG substrate. These spectra are plotted as a function of final-state energy above E_F. In Fig. 4, the final-state energy of 6.2 eV corresponds to the highest final-state, with two-photon energy above E_F. As shown in Fig. 4, the 2PPE spectral features are definitely different among the HOPG substrate and ODT-passivated Ag nanoparticles on the HOPG substrate. The 2PPE spectrum of HOPG substrate reflects the vanishing semimetallic density of states toward the E_F, however, that of ODT-passivated Ag nanoparticles on the HOPG substrate exhibits a clear Fermi-edge at a final-state energy of 6.2 eV. An important point to note is that the 2PPE intensity of ODT-passivated Ag nanoparticles is about two orders of magnitude higher than that of HOPG substrate. The optical extinction spectrum of the present ODT-passivated Ag nanoparticle exhibits the broad Mie plasmon resonance around 3 eV in photon energy. The present exciting laser light with photon energy of 3.1 eV resonantly excites the Mie plasmon in Ag nanoparticles. Therefore, it is considered that the 2PPE yield from

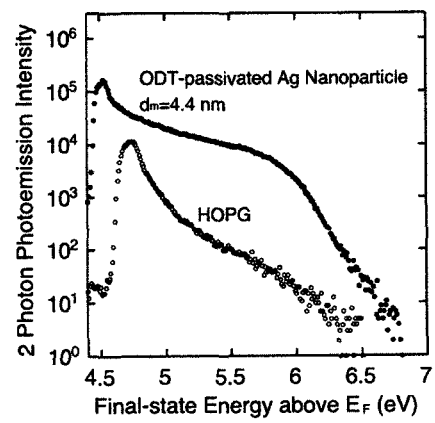

Fig. 4. 2PPE spectrum of ODT-passivated Ag nanoparticles on HOPG substrate with mean diameter of 4.4 nm at room temperature measured with exciting photon energy of 3.1 eV at zero pump-probe delay. The lower spectrum shows the 2PPE spectrum observed for HOPG substrate for a comparison. The spectra are plotted as a function of the final-state energy above E_F.

ODT-passivated Ag nanoparticles enhances due to the local field enhancement by excitation of Mie plasmons localized in the Ag nanoparticles and the observed 2PPE spectrum dominates the 2PPE signals from the ODT-passivated Ag nanoparticles. This indicates that the present 2PPE measurements allow us to distinguish between 2PPE from the Ag nanoparticles and HOPG substrate and to selectively investigate the dynamics in the Ag nanoparticles even at the present heterogeneous sample surfaces.

Interferometric two-pulse correlation (I2PC) measurements were carried out by measurements of photoemission intensities at the given photoelectron energy while interferometrically scanning the pump-probe delays. Figure 5 shows the I2PC at different final-state energies of ODT-passivated Ag nanoparticles on the HOPG substrate with a mean diameter of 4.4 nm. The I2PC signals as shown in Fig. 5 can be decomposed into the phase-averaged signal, and envelopes of ω- (laser frequency) and 2ω-oscillating components.[14] The phase-averaged signal, and ω- and 2ω-envelopes provide the energy relaxation of the intermediate state, and phase relaxation among initial, intermediate, and final state involved two-photon photoemission process. The focus of this paper is on the energy relaxation time T_1 which is obtained from the phase-averaged signals of I2PC. From the detailed analyses of I2PC in Fig. 5, it is found that the energy relaxation times are significantly larger than that of the bulk Ag crystallite. While the energy relaxation time at excited-state energy of about 3 eV for bulk Ag crystallite is less than 10 fs,[15] the energy relaxation time of the present ODT-passivated Ag nanoparticles at same excited-state energy is about 20 fs. However, the present I2PC has been observed under the Mie plasmon resonance condition. This collective excitation (Mie plasmon excitation) results in an internal field enhancement, which can last much longer (depending on the plasmon damping time) than the laser pulse. In other words, the internal effective field that is responsible for the photoemission, is much stronger and temporal broadened compared to the incident laser field. That will result in a broadened I2PC trace. Therefore, the present I2PC traces include the both contributions of intermediate states (single-particle excitation) and plasmon (collective excitation) dynamics. In order to distinguish the both contributions, we are calculating the temporal dynamics of the Mie plasmon in the Ag nanoparticle based on the finite difference time domain (FDTD) method.

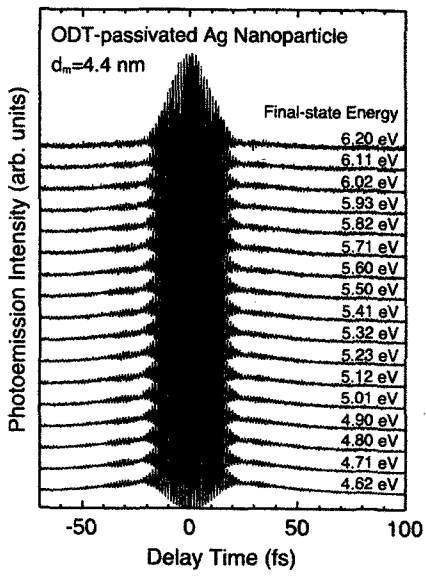

Fig. 5. I2PC at different final-state energies above E_F of ODT-passivated Ag nanoparticles on HOPG substrate with a mean diameter of 4.4 nm at room temperature measured with exciting photon energy of 3.1 eV. The final state energy relative to Fermi level is indicated on each I2PC.

ACKNOWLEDGEMENT

The author thanks H. Sasaki, T. Nagasawa, Y. Takeda, M. Imamura, and S. Sato of Tohoku University, K. Takahashi and T. Ito of Institute of Molecular Science, K. Onda and H. Petek of University of Pittsburgh for help in the experiments, and M. Haraguchi of Tokushima University for useful discussions. This work was supported by grants from the Ministry of Education, Culture, Sports, Science and Technology of Japan (Grant-in-Aid for Young Scientists (A) and Grant-in-Aid for Scientific Research for Priority Areas).

REFERENCES

[1] M. P. A. Viegers and J. M. Trooster, *Phys. Rev. B* **15**, 72 (1977).
[2] G. Medeiros-Ribeiro, D. A. A. Ohlberg, R. S. Williams, and J. R. Heath, *Phys. Rev. B* **59**, 1633 (1999).
[3] M. Brust, M. Walker, D. Bethell, D. J. Schiffrin, and R. Whyman, *J. Chem. Soc., Chem. Commun.* **1994**, 801 (1994).
[4] M. M. Alvarez, J. T. Khoury, T. G. Schaaff, M. Shafigullin, I. Vezmar, and R. L. Whetten, *Chem. Phys. Lett.* **266**, 91 (1997).
[5] A. Taleb, V. Russier, A. Courty, and M. P. Pileni, *Phys. Rev. B* **59**, 13350 (1999).
[6] W. D. Luedtke and U. Landman, *J. Phys. Chem.* **100**, 13323 (1996).
[7] A. Tanaka, Y. Takeda, T. Nagasawa, and S. Sato, *Phys. Rev. B* **67**, 033101 (2003).
[8] X. M. Lin, C. M. Sorensen, and K. J. Klabunde, *J. Nanoparticle Res.* **2**, 157 (2000).
[9] M. Seidl, K.-H. Meiwes-Broer, and M. Brack, *J. Chem. Phys.* **95**, 1295 (1991).
[10] H. Hovel, B. Grimm, M. Pollmann, and B. Reihl, *Phys. Rev. Lett.* **81**, 4608 (1998).
[11] H. Hovel, B. Grimm, M. Pollmann, and B. Reihl, *Eur. Phys. J. D* **9**, 595 (1999).
[12] M. G. Mason, *Phys. Rev. B* **27**, 748 (1983).
[13] P. H. Citrin, G. K. Wertheim, and Y. Baer, *Phys. Rev. B* **27** 3160 (1983).
[14] H. Petek and S. Ogawa, *Prog. Surf. Sci.* **56**, 239 (1997).
[15] M. Bauer and M. Aeschlimann, *J. Electron Spectrosc. Relat Phenom.* **124**, 225 (2002).

(Received December 24, 2004; Accepted February 10, 2005)